ELSEVIER

NeuroImage

www.elsevier.com/locate/ynimg
NeuroImage 25 (2005) 206–218

Accounting for nonlinear BOLD effects in fMRI: parameter estimates and a model for prediction in rapid event-related studies

Tor D. Wager,[a,*] Alberto Vazquez,[b] Luis Hernandez,[b] and Douglas C. Noll[b]

[a]*Department of Psychology, Columbia University, 1190 Amsterdam Avenue, New York, NY 10027, USA*
[b]*University of Michigan, Ann Arbor, MI 48109, USA*

Received 19 July 2004; revised 9 October 2004; accepted 2 November 2004
Available online 4 January 2005

Nonlinear effects in fMRI BOLD data may substantially influence estimates of task-related activations, particularly in rapid event-related designs. If the BOLD response to each stimulus is assumed to be independent of the stimulation history, nonlinear interactions create a prediction error that may reduce sensitivity. When stimulus density differs among conditions, nonlinear effects can cause artifactual differences in activation. This situation can occur in rapid event-related designs or when comparing blocks of unequal lengths. We present data showing substantial nonlinear history effects for stimuli 1 s apart and use estimates of nonlinearities in response magnitude, onset time, and time to peak to form a low-dimensional parameterization of these nonlinear effects. Our estimates of nonlinearity appear relatively consistent throughout the brain, and these estimates can be used to form adjusted linear predictors for future rapid event-related fMRI studies. Adjusting the linear model for these known nonlinear effects results in a substantially better model fit. The biggest advantages to using predictors adjusted for known nonlinear effects are (1) higher sensitivity at the individual subject level of analysis, (2) better control of confounds related to nonlinear effects, and (3) more accurate estimates of design efficiency in experimental fMRI design.

Keywords: fMRI; Event-related studies; Nonlinear effects

Introduction

Several studies have demonstrated the existence of nonlinearities in blood oxygen level-dependent (BOLD) fMRI data (Birn et al., 2001; Boynton et al., 1996; Buxton et al., 1998; Friston et al., 2000; Huettel and McCarthy, 2001; Vazquez and Noll, 1998). These nonlinearities are believed to arise from both nonlinearities in the vascular response, believed to be caused primarily by viscoelastic properties of blood vessels (Buxton et al., 1998; Vazquez and Noll, 1998, 2002), and nonlinearities at the neuronal level, such as the adaptive behavior of neuronal activity (Kileny et al., 1980; Logothetis, 2003; Logothetis et al., 2001; Wilson et al., 1984). Models of the underlying physiological changes that induce nonlinearities in the observed signal have been developed, primarily with the goal of understanding the nature of the BOLD response (Buxton and Frank, 1997; Buxton et al., 1998; Vazquez and Noll, 1998). Estimation methods (Cohen, 1997; Friston et al., 1998, 2000) have also been developed that may be used to model nonlinearities in functional experiments.

Nonlinearity is an important issue in the design of experiments, and in the analysis of both blocked and event-related fMRI data under certain conditions (we present some scenarios below). In experimental design, the solution to the optimal stimulus spacing for an event-related design depends on the magnitude of nonlinear stimulus effects (Wager and Nichols, 2003). In a truly linear system, the efficiency of detecting a difference between conditions (e.g., Task A–Task B) increases without bound as the interstimulus interval approaches zero (e.g., Josephs and Henson, 1999), which is clearly not true of BOLD data (discussed further in Wager and Nichols, 2003). The true sensitivity is limited by nonlinear saturation in the BOLD signal, and to develop maximally sensitive experimental designs we must have a reasonably accurate model of the saturation. Virtually all work on experimental fMRI design assumes linear responses (Birn et al., 2002; Liu, 2004; Liu and Frank, 2004; Liu et al., 2001; Mechelli et al., 2003), or at least a very simple nonlinear model (Wager and Nichols, 2003), and would benefit from a simple approximate characterization of expected nonlinear responses.

Nonlinear effects are largely ignored in neuroscientific and psychological studies using BOLD fMRI due possibly to several reasons. First, the finding that BOLD responses were approximately linear over a range of stimulus durations promised to greatly simplify analysis (Boynton et al., 1996). Nonlinearities are believed to be relatively small compared to the overall BOLD effects for events spaced more widely than 2 s (Buckner, 1998), although some studies have found fairly substantial saturation effects (17–25%) at 5 s (Miezin et al., 2000). Second, most work on development of expected hemodynamic responses has focused on determining canonical responses to single stimuli rather than

* Corresponding author.
E-mail address: tor@psych.columbia.edu (T.D. Wager).
Available online on ScienceDirect (www.sciencedirect.com).

1053-8119/$ - see front matter © 2004 Elsevier Inc. All rights reserved.
doi:10.1016/j.neuroimage.2004.11.008

exploring interactions among them. Finally, existing models such as the Volterra series (Friston et al., 1998, 2000) require fitting a large number of parameters, which may not be practical for many multicondition fMRI experiments due to overfitting and loss of power. In addition, the interpretation of parameter estimates with such models becomes more problematic.

Nonlinearities in the BOLD response may be of more practical concern for neuroscientists and psychologists than is generally recognized. They pose the biggest problem in rapid ER designs, which have become much more popular in the literature due to their potential for more specific psychological and neuroscientific inference, including linking BOLD activity to specific psychological events within trials and estimating the relative latency of responses to different events (Henson et al., 2002; MacDonald et al., 2000; Miezin et al., 2000; Wagner et al., 1998). In a rapid ER design, events of various types are presented in random or pseudo-random order, and temporal stochasticity is often introduced into the design. Ignoring nonlinearities in several experimental scenarios could have severe negative consequences for the validity of the study. We expand briefly on several of these scenarios below.

Scenario 1: comparing blocks of different lengths or events in rapid designs that are not carefully balanced

In a simple, periodic task–control block design, the shape and overall magnitude of the BOLD response to a stimulation block of closely spaced events is highly determined by nonlinearities in the BOLD response. Correctly modeling the shape of the response to a stimulation block requires a model of nonlinear effects. If the blocks are of equal durations, the expected nonlinearities are also equivalent and do not pose a serious problem; but if blocks are of unequal durations, problems in interpreting activations can arise. If blocks are of unequal durations (e.g., 20 s periods for condition A, and 10 s periods for B), differences in the nonlinear contribution to measured responses in each block can produce artifactual activations. Because the magnitude of the observed BOLD signal is a nonlinear function of both the time on task and the magnitude of neuronal responses, and if the time on task is not matched, it becomes very difficult to interpret observed BOLD differences in terms of neuronal activity differences. This problem is alluded to in discussions of "duty cycle," which highlight the difficulties in making inferences if the time on task is not known (Hernandez et al., 2002). A concrete illustration of how false-positives may be created and how the same principle applies to rapid ER designs is provided in the discussion and in Fig. 7.

Scenario 2: comparing temporally adjacent periods

Many investigators study processes that are extended in time, such as working memory (e.g., D'Esposito et al., 1999; Haxby et al., 2000). In a working memory trial, stimuli are typically presented for study, and participants must maintain memories of these stimuli over a delay interval. A typical frontal cortex response looks like a large rise following study, which decreases and plateaus during the delay interval (Haxby et al., 2000). Is the region responsive during study, maintenance, or both? Is it more responsive during study than maintenance, as the largest BOLD signal change immediately follows study? Without a good model of nonlinearity, it is impossible to interpret the relative magnitudes of the study- and delay-related signals.

Scenario 3: individual activation and individual differences

Rapid ER designs may offer a substantial increase in detection power for individual subjects, even when nonlinearities are not accounted for (Burock et al., 1998). A simple nonlinear model could further provide increased detection sensitivity in individual participants by providing better fits to time course data. In addition, accounting for nonlinear effects may provide more accurate estimates of an individual's true response magnitude, improving the accuracy of correlations between activation and performance across participants. (The latter is true primarily when the stimulus sequences, and thus nonlinear effects, differ across individuals.)

Scenario 4: comparing subpopulations of trials separated post hoc

Another case in which nonlinear effects should be accounted for is when performance in an ER-fMRI design is correlated with brain activation on a trial-by-trial basis, or trials are otherwise separated on the basis of performance. Recent examples come from the literature on cognitive interference (e.g., Kerns et al., 2004) and success of long-term memory encoding (e.g., Davachi and Wagner, 2002). In these cases, estimates of response magnitude to individual trials or subpopulations of trials are expected to be much more accurate if nuisance effects due to stimulation history are parsed out. In addition, confounds due to stimulation history can be avoided.

As an example, suppose a researcher is interested in trial–history effects (e.g., Kerns et al., 2004)—that is, whether the magnitude of activation on a trial (X) depends on whether preceding trials were of type I or C. Thus, the researcher's hypothesis is that the neural response to X is greater for C–X than I–X. Linear modeling, either with a known HRF shape or deconvolution, assumes that the responses to the preceding trial (C or I) can be separated from the response to X, and any observed BOLD differences in X are neural and of psychological interest. However, what happens if the response to I is greater than to C, and that response carries over to produce nonlinear saturation in the response to X? Such effects can be substantial (17–25%) for trials spaced as far as 5 s apart (Miezin et al., 2000). In this case, nonlinearities would decrease responses to I–X more than C–X, creating a C–X > I–X effect. Kerns et al. (2004) tested just such a hypothesis with trials spaced 3 s apart. They found the expected effect, C–X > I–X, in a region of anterior cingulate cortex known to show I > C responses (MacDonald et al., 2000). Thus, it is reasonable to ask whether the observed effects were neural or vascular in origin. In experimental paradigms for which this confound cannot be removed by altering the design, incorporating a good model of nonlinearity into the analysis can help ameliorate the problem.

The current study

In this paper, we attempt to characterize nonlinear effects in visual and motor cortex as an empirical function of stimulus history. We find substantial nonlinearities in the magnitude, peak delay, and dispersion of the hemodynamic response at an ISI of 1 s, which poses a serious problem for rapid ER designs at short ISIs. We find that these nonlinear effects are relatively consistent throughout the brain areas tested and develop a set of linear equations approximating their form. These equations are used to create a modified convolution that allows the response magnitude,

onset delay, and peak delay to vary as a function of the position of the stimulus relative to others of the same type. Thus, as in forms of linear modeling in common practice (e.g., Friston et al., 1995a), one linear predictor for each event type is fit to the data; but our predictors are constructed taking into account nonlinear interactions of the form we observe experimentally. In essence, this process is a low-dimensional parameterization of nonlinear effects. The modified predictors can then be used in the GLM framework (e.g., Friston et al., 1995b), producing a more accurate prediction of the response than the prediction provided without accounting for nonlinearity.

We find that the adjusted linear model is more accurate than the standard GLM at capturing the variation in the observed signal. In addition, it can be used to provide more meaningful predictions of the response to a continuous stimulation epoch that are less dependent on an arbitrary chosen sampling resolution.

Methods

Tasks and data collection

Twelve students at the University of Michigan were recruited and paid US$50 for participation in the study. All human participants procedures were conducted in accordance with Institutional Review Board guidelines. One participant failed to show visual activation to a positive control (debriefing revealed that he was extremely sleepy) and was excluded from further analysis. One participant showed atypical visual and motor hemodynamic responses that were not fit well by the canonical model and was excluded from nonlinearity analyses, leaving a final sample of $n = 10$.

Participants performed two visual–motor tasks in which they observed contrast-reversing checkerboards (16 Hz) and made manual button-press responses. In the first task (localizer), blocks of unilateral contrast-reversing checkerboards were presented on an in-scanner LCD screen (IFIS, Psychology Software Tools). Data were collected in a single functional run comprising 10 blocks of 16 s each of alternating left and right hemifield stimulation. Subjects made motor responses continuously with the index and middle fingers of the ipsilateral hand; thus, when the checkerboards appeared on the left of fixation, participants responded with the left hand and vice versa for the right-hemifield checkerboards. Results were used to localize primary visual and motor cortices in each hemisphere for each subject.

The main task consisted of eight functional runs of visual/motor stimuli. In each run, a series of brief contrast-reversing checkerboard stimuli (250 ms stimulus duration) separated by a 1-s stimulus–onset asynchrony (SOA) were observed by participants. Stimuli were as close to full field as the stimulus presentation system allowed (approximately 30° of visual angle). Participants were instructed to press the index and middle fingers of both hands together each time they saw a checkerboard stimulus. Each stimulus series consisted of either 1, 2, 5, 6, 10, or 11 stimuli separated by 1 s, followed by 30 s of rest. The order of the six series types (i.e., series of 1, 2, 5, 6, 10, or 11 stimuli) was counterbalanced across runs, and two trials of each train length were presented in each run, for a total of 16 trials per series length for each participant.

Spiral-out gradient echo images were collected on a GE 3T fMRI scanner (Noll et al., 1995). Seven oblique slices were collected through visual and motor cortex, 3.12 × 3.12 × 5 mm voxels, TR = 0.5 s, TE = 25 ms, flip angle = 90, FOV = 20 cm.

Data analysis

Data from all images were corrected for slice–acquisition timing differences using a four-point sinc interpolation (Oppenheim et al., 1999) and corrected for head movement using a six-parameter affine registration (Woods et al., 1998) prior to analysis.

Determining ROIs

Data from the localizer task were used to derive visual and motor regions of interest (ROIs) for each participant. For each participant, data were analyzed using SPM99 (Friston et al., 1995a; no global scaling, high-pass filter 100 s, no low-pass filter). Statistical maps comparing left > right and right > left visual hemifield stimulation (with corresponding concurrent left- or right-hand motor responses) were thresholded at $t > 3.5$ (approximately $P < 0.0003$).

For each map, the largest region of contiguous suprathreshold voxels surrounding the calcarine fissure (for visual cortex) or the precentral gyrus (for motor cortex) in the hemisphere contralateral to stimulation was saved as a region of interest (ROI). Subsequent analyses were performed on the average activity within these regions (Fig. 1).

Time series analysis and HRF fitting

For the analysis of the main task, average time courses across voxels in each of the four regions were extracted for each subject. Time courses were mean centered within each run, concatenated across runs, and high-pass filtered using the method

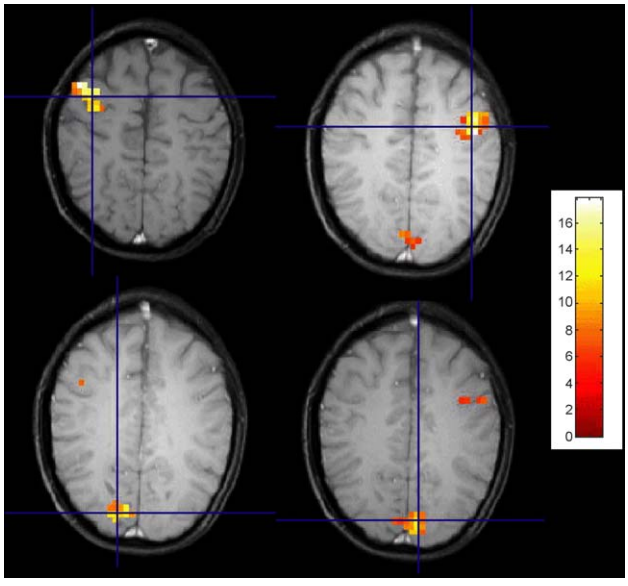

Fig. 1. Representative motor and visual activations from the localizer task (top and bottom panels, respectively) for a representative participant selected at random. The left panels show activation for the contrast [right stimulation > left stimulation], and the right panels show activation for [left stimulation > right stimulation]. The left side of each slice is the left side of the brain. The color bar shows t values for activation reliability. The activation threshold was $t > 3.5$. Each of the 11 participants showed activation in left and right visual and motor cortex at this threshold, and these activations were used as regions of interest in the main task.

of SPM99 at 0.0118 Hz (85 s). Individual observations were excluded that were more than three standard deviations from the mean of the filtered time series. Activity was averaged across trials of each series type, omitting outlier values casewise, for each ROI (Fig. 2).

To compare series of different lengths, difference waveforms for three comparisons—2 stimulations vs. 1, 6 vs. 5, and 11 vs. 10—were calculated. These difference waveforms represent the residual signal of the 2nd, 6th, and 11th stimulus in the sequence. A canonical hemodynamic response function (implemented in SPM, http://www.fil.ion.ucl.ac.uk/spm/ (Friston et al., 1995b), with free parameters for magnitude (height), onset delay, and time to peak, was fit to the difference waveforms for each pair of conditions to determine the residual magnitude, onset delay, and peak delay of the response to the *n*th stimulus (i.e., 2nd, 6th, or 11th). Fitting was performed with the Levenberg–Marquardt method (Press et al., 1992; Miezin et al., 2000).

The resulting parameter values for height, onset time, and peak delay were averaged across subjects to obtain group estimates for each ROI. These parameter estimates varied as a function of the position of the stimulus in the series, indicating that height, onset time, and peak delay are nonlinear with respect to stimulation history. HRF parameter estimates for each condition within participant were analyzed using factorial repeated measures ANOVA, with functional region (visual vs. motor), hemisphere (left vs. right), and stimulus position in series (1st, 2nd, 6th, or 11th) as factors.

We chose to approximate the form of these nonlinearities across regions using a biexponential model, which provides a canonical, mathematical description of the nonlinearity (one can think of this as choosing an exponential basis set to describe the nonlinear behavior in height, onset, and peak delay of the HRF). Thus, a biexponential function was fit to the average extracted parameter estimates across participants and brain regions (Fig. 4B), using a standard nonlinear least squares algorithm (lsqcurvefit.m) in Matlab 6.1. The function was of the form:

$$y = Ae^{-\alpha x} + Be^{-bx} \quad (1)$$

with free parameters A and α, B and β describing the scaling (allowed to be positive or negative) and exponent of two exponential curves. The fitted biexponential curve describes the nonlinear change in BOLD magnitude, onset time, and peak delay as a function of stimulation history.

We found that a biexponential model was necessary to fit the data, as onset and time to peak parameters varied nonmonotonically with stimulus history; a single exponential model is always monotonic and is therefore inadequate. Although a monoexponen-

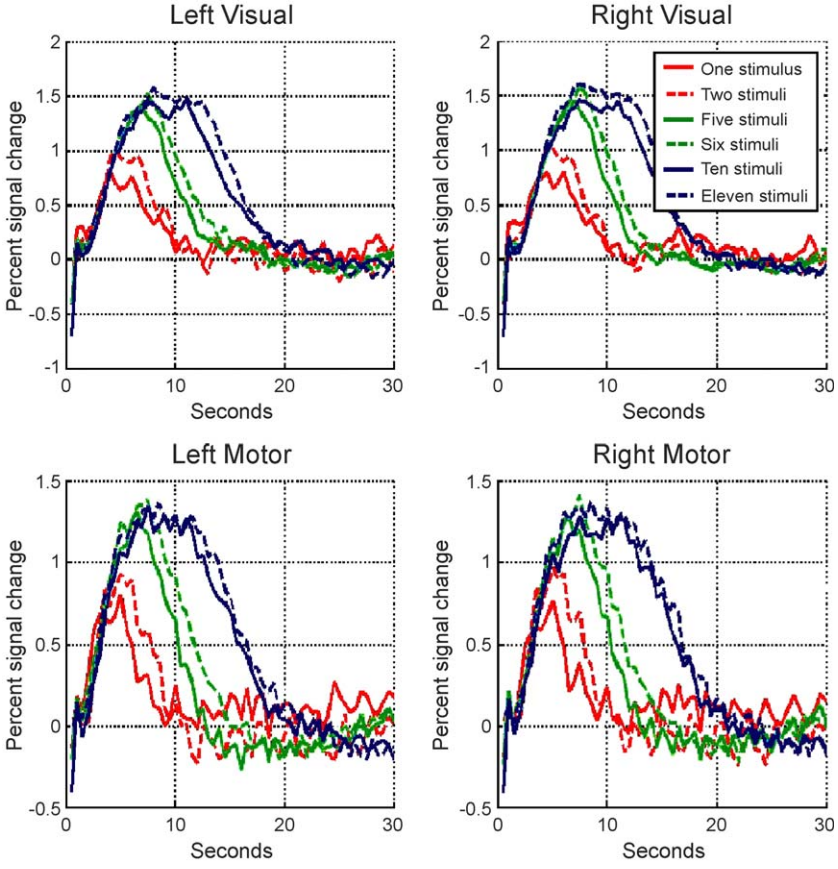

Fig. 2. BOLD responses averaged across trials and participants for each region of interest. Responses to series of one or two visual stimuli are shown in red solid or dashed lines, respectively, and the difference between these waveforms was used to estimate the residual response to the second stimulus. Residual responses to the 6th and 11th stimulus in a series were estimated by subtracting the solid from the dashed green (sixth) and blue waveforms (eleventh), respectively. Subtractions were performed on individual trial-averaged data, and the error across participants was used as the error term in statistical analyses of nonlinearity (e.g., a "random effects" analysis). The high-frequency noise observable in the waveforms is centered around 1 Hz and is likely due to heartbeat-related pulsatility that would be aliased into the task frequency at longer TRs.

tial curve might be adequate for the height parameter, we were concerned with accurately predicting the form of the response rather than fitting the simplest possible model, so the biexponential model is a better choice. Two advantages of the biexponential are that it provides both a good fit to the data and reasonable values if extrapolated beyond the range of data collected. The fits asymptote at 0 or some constant value as stimulus position approaches infinity. This property is physiologically plausible: the effects of stimulus position in the series will become negligible as the physiological system evolves toward steady state. That is, if there have been no recent stimuli, a stimulus will affect BOLD responses to successive ones, but if stimulation has been occurring for a long time (e.g., 1 min), one additional second of stimulation will have little effect on ensuing BOLD responses. (This simplification, however, may cause the model to underestimate the BOLD response with such long stimulation times; thus, the model is most useful for event-related designs and shorter epochs.) For time to peak, the model was fit to centered data and the mean time to peak was added as a constant to the equation; thus, the time to peak approaches the canonical HRF value as the system approaches steady state (Fig. 3).

Comparison of nonlinear with linear model and balloon model

To compare the impact of observed nonlinearities on model fits, we used a modified linear convolution that takes into account stimulation history. The linear regressors of this model were constructed by adjusting the height, time to onset, and time to peak of the predicted HRF for each stimulus using the equations produced by the biexponential fitting (see Results). We compare this 'adjusted' linear model against two benchmarks, the standard linear model and the predicted response of the balloon model (Buxton et al., 1998; Friston et al., 2000; Figs. 5 and 6), as well as the standard linear model in terms of their mean squared error (MSE). The balloon model was fit to the aggregate data using a nonlinear least squares algorithm in Matlab (Mathworks Inc., Natick MA). The blood flow response amplitude, duration, and delay were designated as free parameters of the model, in addition to a blood volume hysteresis parameter and a BOLD response amplitude parameter.

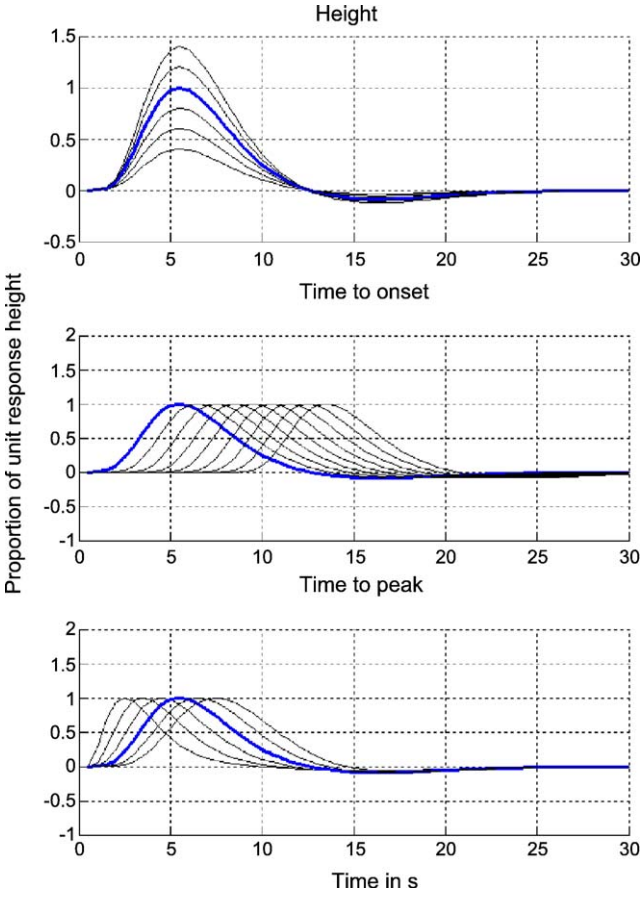

Fig. 3. Effects of varying predicted hemodynamic response (HRF) height (top panel), time to onset (middle panel), and time to peak (bottom panel) of the canonical SPM99 HRF. An HRF with these three free parameters was fit to trial-averaged data using nonlinear least squares. Starting estimates are the default SPM99 values, shown in blue. Time to onset and time to peak are not orthogonal, but together they capture much of the observed variability in HRF latency and width. Fits with more free parameters (e.g., dispersion, height-to-undershoot ratio) were obtained, but they contributed little additional explanatory power and are not further reported.

Results

Visual and motor activation

In the blocked localizer run, all subjects showed activity in discrete regions of visual cortex (around the calcarine fissure) and motor cortex (in the precentral sulcus/gyrus) at the threshold of $t > 3.5$. As expected, right hemisphere activations were produced by the left > right stimulation comparison, and vice versa for left hemisphere activations. These four regions (right and left visual and motor regions) were used as ROIs in the event-related analysis.

The average responses in each region for each trial type, a stimulus series of either 1, 2, 5, 6, 10, or 11 stimuli, across trials and participants are shown in Fig. 2. In the figure, solid lines show responses for trains of 1, 5, and 10 stimuli. Dashed lines show responses for 2, 6, and 11 stimuli.

Estimates of nonlinearity

Results for ANOVA on response magnitudes showed that the first stimulus produced the largest response, with each successive stimulus position tested producing a smaller activation. Percent signal changes were 0.66%, 0.44%, 0.33%, and 0.20% for the 1st, 2nd, 6th, and 11th events. The main effects of stimulus position ($F = 11.73$, MSE = 2.02, $P < 0.001$ with Huynh–Feldt correction for nonsphericity) and linear trend in stimulus position ($F = 31.27$, MSE = 5.04, $P < 0.001$) were significant. Due to the unequal intervals chosen for stimulus position (1st, 2nd, 6th, and 11th), the linear trend actually signifies a nonlinear (e.g., exponential) decrease in response magnitude as a function of prior stimulation history. The trend could equivalently be interpreted as larger than expected activation for brief events (Birn et al., 2001), but we prefer to frame the effects in terms of smaller activations for repeated events (response saturation), reflecting an underlying neural and/or vascular hysteresis (Buxton and Frank, 1997; Vazquez and Noll, 1998).

No other main effects or interactions were significant (max F across all other effects = 2.03, $P = 0.18$), with the exception of quadratic trends in the region × stimulus position ($F = 3.84$, $P = 0.07$) and hemisphere × stimulus position ($F = 4.04$, $P = 0.06$) interactions. These effects suggest that in visual cortex, the response decreased more than in motor cortex for the second

stimulus compared to the first, but that the asymptotic value was slightly higher than in motor cortex, as shown in Fig. 4A. Overall, the results show a reasonable degree of consistency across brain regions—the main effects of saturation are much larger than the interactions between saturation and region—indicating that a general model across brain regions could be formulated.

Because our primary goal was to accurately estimate parameters rather than test significance, we estimated onset and

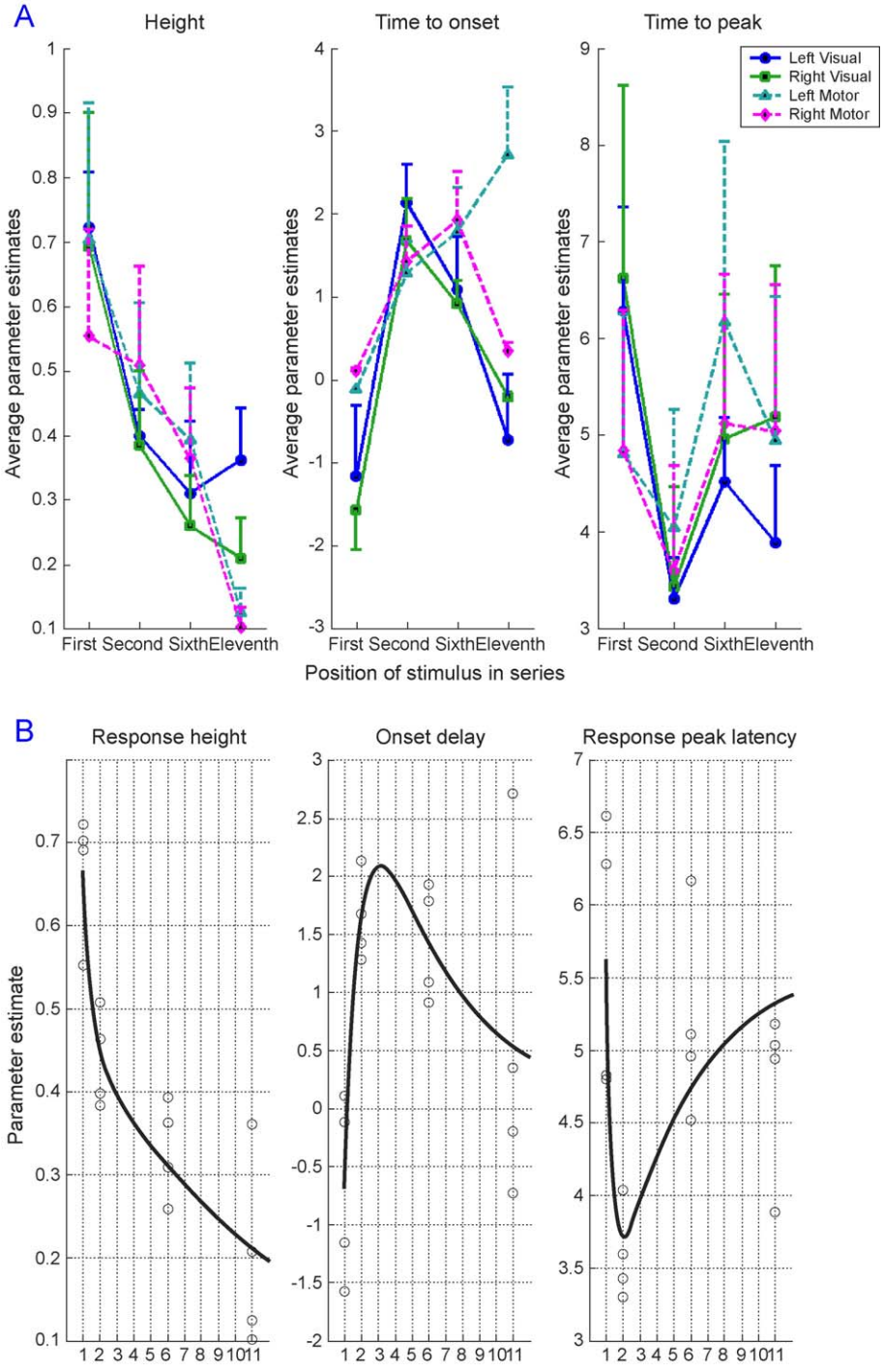

Fig. 4. (A) Parameter estimates for height (left panel), time to onset (middle), and time to peak (right panel) in percentage of signal change (y-axis) as a function of position in the stimulus series (x-axis) in each of the four ROIs (lines). Error bars show the standard error of the mean across participants, which are generally larger than the error for within-subjects comparison across stimulus position. Nonlinear effects (i.e., effects of position, x-axis) are large and relatively consistent across areas, with small but significant differences between visual and motor regions. Because time to onset and time to peak are not orthogonal, their parameter estimates are negatively correlated and display reciprocal behavior (one is high when the other is low), and so these estimates are only meaningful when used together. (B) Parameter estimates for each ROI (circles) and exponential fits to parameter estimates (solid lines). The fits are graphical descriptions of the equations (see text) used to provide a general model of nonlinear effects.

peak delay parameters only for conditions within participants showing significant activation to the nth stimulus (e.g., 6 vs. 5 stimuli produces a positive BOLD activation), on the basis that estimating response delay is not meaningful if there is no significant activation. The delay parameters that could be meaningfully estimated were used in prediction, and mean values for onset and peak delay are shown in Fig. 4A. The resulting missing values in the data set made ANOVA analysis of delay difficult, as there were not enough cases (10 subjects) with valid latency estimates for all conditions (4) in all regions (4), which may cause overestimation of the degrees of freedom. However, for completeness, we report ANOVA results here with missing values replaced with across-subjects means.

ANOVA results for onset delay showed a later onset delay for motor regions than visual ones, as expected (F = 6.51, MSE = 5.66, $P < 0.03$), a nonmonotonic effect is stimulus position (F = 4.79, MSE = 10.23, $P < 0.01$), and an interaction between visual/motor region, hemisphere, and stimulus position (F = 4.86, MSE = 2.70, $P < 0.03$) caused by the late onset for left motor cortex after prolonged stimulation (Fig. 4A, center panel). No other effects were significant. Results for time-to-peak showed a significant interaction between visual/motor and hemisphere (F = 7.69, MSE = 1.14, P = 0.02), with later time-to-peak for motor than visual regions only in the left hemisphere. No other effects were significant, although the effect of stimulus position showed a trend (F = 2.75, P = 0.06). The nonmonotonic effects of delay and time-to-peak in opposite directions suggests that the effects may be related to collinearity between the regression parameters for onset delay and time to peak. Thus, fitted responses for later stimuli in a sequence tend to begin later and rise slightly faster, but the result is little overall change in the delay of the response.

Equations for predicted nonlinearity

Biexponential fits to the nonlinearity estimates are shown in Fig. 4B. Three equations were derived that predict relative BOLD magnitude, onset delay, and peak delay as a function of stimulation history (of repeated brief 1 s stimulations). All of these equations give parameter values as a function of the stimulus position in a sequence of stimuli, and they are given below:

$$m = 1.7141e^{-2.1038x} + 0.4932e^{-0.0770x} \quad (2)$$

$$d = -13.4097e^{-1.0746x} + 4.8733e^{-0.1979x} \quad (3)$$

$$p = 37.5445e^{-2.6760x} - 3.2046e^{-0.2120x} + 5.6344 \quad (4)$$

where m is the stimulus magnitude, as a proportion of the canonical HRF height with no stimulation history, d is the onset delay of the canonical SPM99 HRF in s, and p is the time to peak of the BOLD response in s. These equations constitute the core of our predictive model, and we use these equations to perform a modified convolution of the stimulus sequence as a function of prior stimuli that have recently occurred. The full form of the hemodynamic response, which assumes the shape of the difference of two gamma functions using modified shape (p) and offset (d) parameters, is:

$$f(t) = \frac{m(x)}{\max\left[\frac{(t-d(x))^{p(x)-1}e^{-\lambda t}}{\int_0^\infty t^{p(x)-1}e^{-\lambda}dt}\right]} \times \left(\frac{(t-d(x))^{p(x)-1}e^{-\lambda t}}{\int_0^\infty t^{p(x)-1}e^{-\lambda}dt} - \frac{1}{6}\left(\frac{(t-d(x))^{15}e^{-\lambda t}}{\int_0^\infty t^{15}d^{-\lambda}dt}\right)\right) \quad (5)$$

where t is the time following stimulus onset at some arbitrary divisor of the TR (e.g., 16 samples per TR); x is the position in the stimulus sequence (e.g., 1 is the first time a stimulus occurs in a given time frame); and λ is a constant scaling parameter equal to the TR / the sampling resolution. The first term is a scaling parameter for the magnitude of the response. The second term describes the gamma function for the positive BOLD response, normalized by its integral, minus the gamma function describing the undershoot (scaled to 1/6 the height of the positive response and also normalized).

This function is identical to that implemented in SPM in spm_hrf.m, with p as the first input parameter and d as the sixth, except that the gamma shape and offset parameters d and p are allowed to vary nonlinearly as a function of x. An implementation that uses the nonlinearity parameters described here is available from the authors (see author note).

Note that the magnitude parameter (m) asymptotes at 0 for large x. Therefore, our approximations predict a zero response magnitude for long blocks of stimulation. Because of this, and because the frequency of neural responses is unknown for blocks of continuous stimulation, these equations may not be appropriate for modeling long block designs (e.g., >30 consecutive stimuli).

Modified linear compared with linear and balloon model predictors

Fig. 5A shows the predicted responses for three models: the linear (green line), balloon (blue line), and modified linear (using Eqs. (2)–(4); red line). The critical difference between the linear and other models is the relative predicted response magnitude of short stimulus trains (e.g., one or two stimuli followed by rest) compared with long trains (e.g., 10 or 11 stimuli). The linear model predicts that the relative height of these will differ by a factor of approximately 4.6. After adjusting for observed nonlinearities using the equations (red line), the relative predicted height differs by a factor of approximately 2.3. The balloon and modified linear models agree closely, although the rise time for the balloon model is somewhat faster.

Fig. 5. (A) Predicted responses to stimulation in the first 4 min of the main experiment for the linear model (green), the modified linear model using our nonlinearity estimates (red), and the balloon model (blue). Deflections show the predicted responses to series of 1, 2, 11, 10, 6, 5, 2, and 1 visual stimulus, in that order. Of interest is the relative magnitude of the responses to stimulation series of different lengths. (B) Model fits to the group-averaged data (black line) for the three models to the same series as in A. Vertical black lines below the fits show the stimulation onsets. The linear model underfits the response to brief trains (one or two stimuli) because the relative heights of short and long trains are not captured well by the linear model. Both adjusted and balloon fits are more accurate. (C) Panels show the group average data (top left) and model fits (remaining panels) averaged over all stimuli of a particular series length, as in Fig. 2. The length of each series is shown in the legend. The GLM predictors (top right) underestimate the response to short trains of stimuli.

When the model is adjusted for nonlinearities of the form described in Eqs. (2)–(4), the adjusted linear model provides significantly better fits to the time series data than the linear model. Fig. 5B shows the fits of linear (green line), balloon (blue line), and modified linear (red line) models to the average data across participants (black line) for a randomly selected segment of the

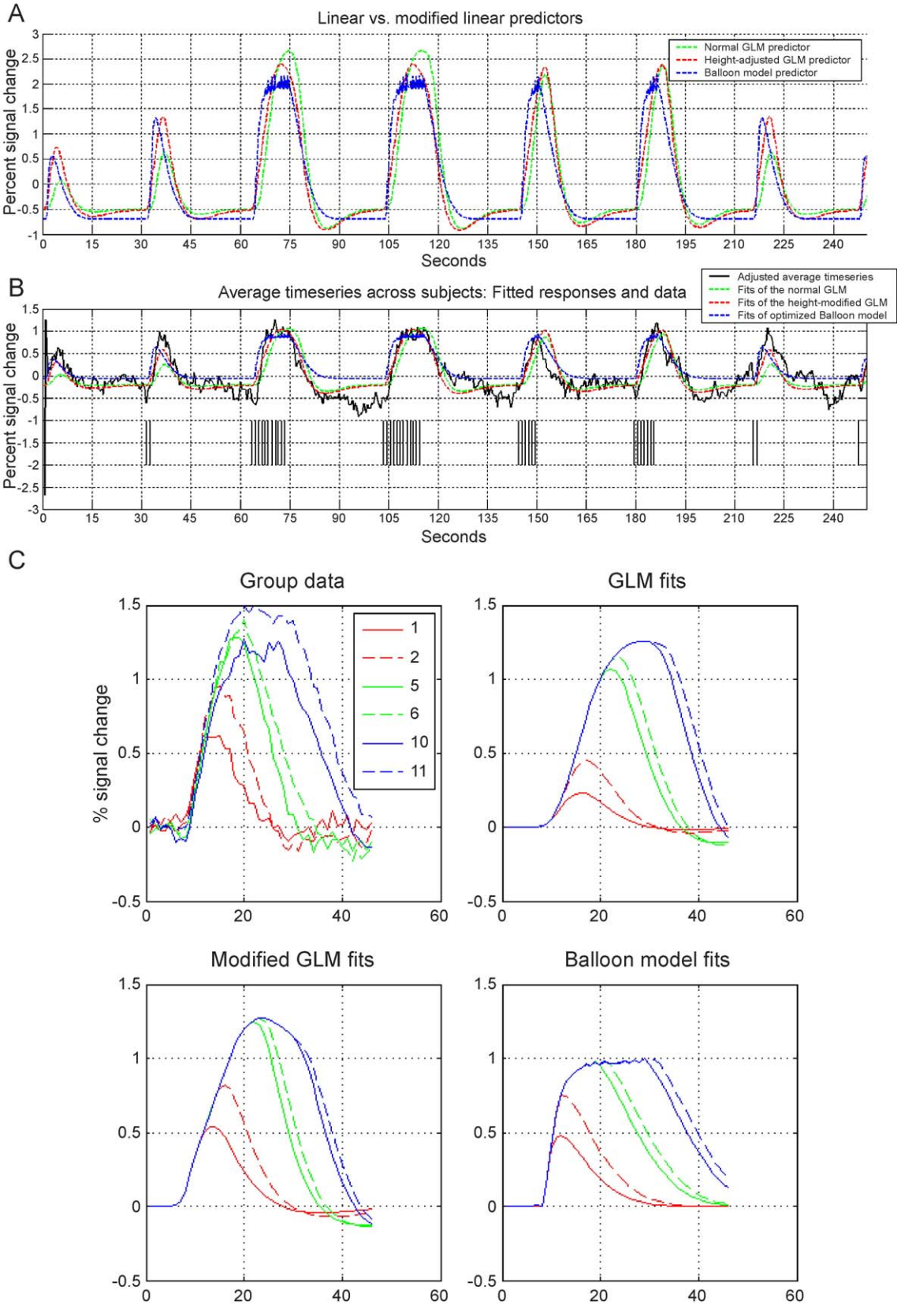

data. Fig. 5C shows the average data across regions (top left panel) and the fits for the GLM (top right), modified GLM (bottom left), and balloon model (bottom right), averaged over series of each length. The figures illustrate that the ordinary GLM fit underfits the response to short series (one- and two-stimulus sequences). We quantified the fits by obtaining the percentage of variance explained (R^2) in fitting both models to the time series data of each participant in each region and taking as a quality measure the R^2 for the adjusted model divided by the R^2 for the linear model. Ratio values over 1 indicate a better fit for the adjusted model. The data are shown in Fig. 6A, which shows that the adjusted model fits better in 41 out of 44 ROIs tested. Benefits in motor cortex were more variable than in visual cortex, but on average, the adjusted model provided approximately a 125% improvement in R^2 over the linear model. The balloon model provided similar fits, with a 121% improvement in R^2 over the linear model (Fig. 6B).

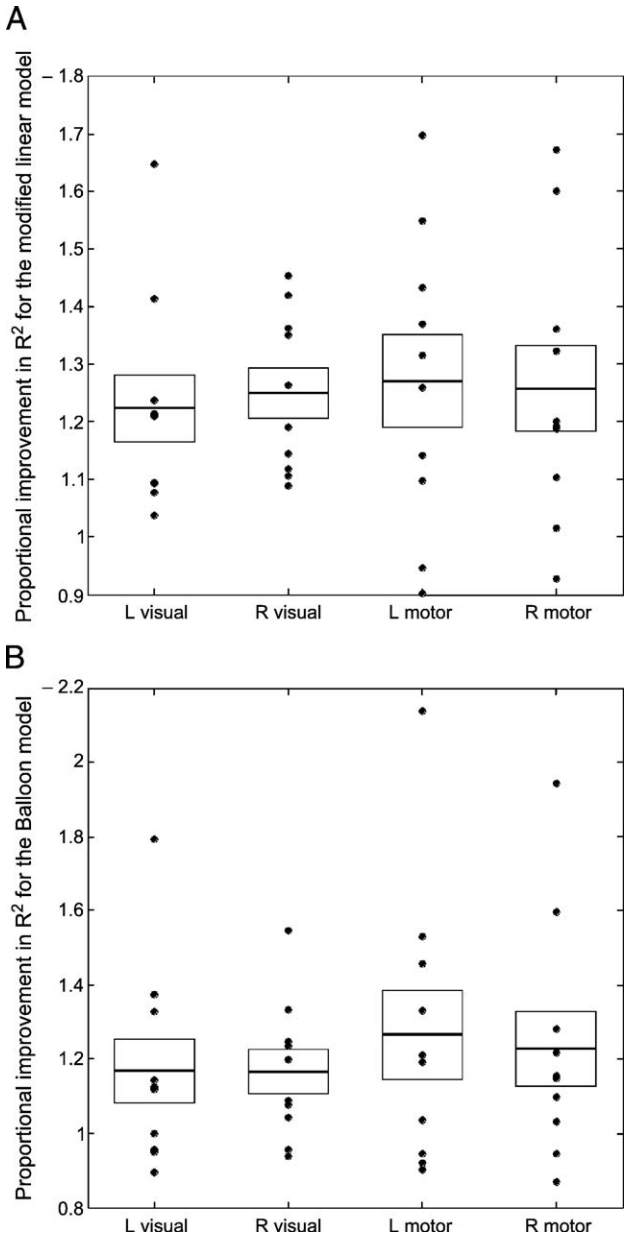

Fig. 6. (A) Proportional improvement in explained variance (R^2, y-axis) by the modified linear model compared to the ordinary linear model for each region of interest (x-axis). Dots indicate relative explained variance for one participant in one region, with a value of 1 signifying no advantage to either model, and positive values signifying a better fit to the adjusted model. The adjusted model fit better in 40 out of 44 regions tested. (B) Proportional improvement in explained variance by the balloon model relative to the linear model. The improvement is similar to that in A.

Discussion

Our results show significant nonlinearities in BOLD response as a function of stimulus history. Some of the early analyses of event-related fMRI found some evidence for similar effects but chose to focus on the rough linearity of the response rather than deviations from linearity. For example, Dale and Buckner (1997) found a slightly smaller, later-onset, and less-dispersed response to a second stimulus that occurred 2 s after an initial one but concluded that the responses were roughly linear. Later, Miezin et al. (2000) reported 10% nonlinear reductions in response magnitude after a longer 5-s delay. Our findings that the response is reduced by nearly 50% if preceded by a stimulus 1 s earlier complement these findings and underscore the importance of avoiding potential confounds created by differences in nonlinearity across experimental conditions.

This experiment was motivated by interest in predicting signal nonlinearities for the purpose of avoiding such confounds and improving model fits in psychological experiments. In this task, it is necessary to walk a fine line between predictive power and explanatory power. This classic tradeoff in statistics poses a thorny problem for researchers of all disciplines. While the Volterra series makes accurate overall predictions of the response, multicollinearity between predictors makes the portion of the signal attributable to parameters of psychological interest (such as the signal related to memory encoding, or the difference between shifting and static attention) difficult to estimate reliably.

Our approach was to perform a separate experiment with the goal of obtaining fixed parameter estimates for one type of nonlinearity, nonlinearity induced by stimulation history, for use in the design and analysis of future studies. The strategy consists of building the regressors in the general linear model as nonlinear functions of the stimulus response instead of assuming linearity and performing a convolution of a canonical response function with a stimulus train. In our method, the individual responses are scaled relative to their preceding responses by a canonical, empirically determined set of equations (Eqs. (2)–(4)).

Avoiding false-positives in event-related and blocked designs

One use of these equations is when investigators aim to accurately model responses within individual participants in a rapid event-related design, as when assessing significance levels within individual participants. For a group (i.e., random effects) analysis, accurate modeling of nonlinearities is generally less important. However, there are situations in which inaccurate modeling of nonlinearities (i.e., using the linear model without adjustment) may create biased estimates across participants, leading to false-positives or false-negatives with respect to a true difference in underlying responses across block or trial types. This problem can occur when (1) blocks or epochs of different lengths are compared without accounting for nonlinearities in the response as a function

of stimulation length, or (2) when events are compared that differ in their densities or frequencies of occurrence (if events can occur closer than 2–3 s apart). The following is an example to illustrate a problematic block design. Fig. 7 shows the simulated response to a block design with unequal block durations without taking nonlinearity into account. The "true data," shown in black, is based on the canonical SPM HRF modified using our nonlinearity estimates (Eqs. (2)–(4)). The blue lines are the linear model predictors. The "neural response" underlying both conditions is exactly the same, a unit response every 0.5 s, evenly distributed across both block types. Because the blocks for two conditions to be compared (A and B) are of unequal lengths (10 and 20 s), the predicted height for the longer block is of greater magnitude than the shorter one. When the linear model is fit to the data, it finds a difference in "activity" between conditions A and B (panel 3), corresponding to beta values of 0.30 and 0.25 for A and B. However, this difference is not related to underlying neural activity in A vs. B but rather to inaccuracies in the relative scaling of the two predictors in a model that does not account for stimulation history effects.

This principle also extends to event-related (ER) designs that compare different trial types. In a rapid ER design, events of various types are presented in random or pseudo-random order, and temporal stochasticity is often introduced into the design. These properties produce designs that have groups of uneven numbers of events closely spaced in time. If the trial types differ in their density with respect to time, nonlinear saturation will also differ, and the same neuronal activity to each trial type may translate into different estimates of BOLD response magnitude. At best, the residual error in the model fit will increase. At worst, if the event spacing (and thus the magnitude of nonlinear interactions) differs among event types, analysis may yield false-positive results.

Sources of nonlinearity and prediction of BOLD response

Nonlinearity in BOLD responses can come from a number of sources. At the single neuron level, the firing in response to stimulation varies over time and is usually not a linear or time-invariant function of the stimulus intensity (e.g., Logothetis, 2003). At short (within stimulus) or long (across minutes or days) time delays, habituation and sensitization of neurons to particular stimuli often occur (Kileny et al., 1980; Logothetis, 2002; Wilson et al., 1984). From a psychological point of view, the response to a stimulus can vary based on a number of adaptive mechanisms that result in a nonlinear neuronal firing pattern, including the development of a strategy, learning new information, and changes in attention or alertness during the task (Raichle et al., 1994).

Even in the case of near-linear neuronal responses, the vascular response is clearly nonlinear, an effect attributed to the viscoelastic properties of the blood vessels. Several groups have contributed with theoretical models of nonlinearity based on auxiliary measurements of blood flow, oxygen saturation, and other parameters (Buxton and Frank, 1997; Buxton et al., 1998; Mandeville et al., 1999; Vazquez and Noll, 1998). Perhaps the most popular model is the one presented by Buxton et al. (1998), in which the response is characterized as a function of the oxyhemoglobin quantity in the vessels. The vessels' elastic properties allow their diameter to increase up to a point when there is blood flow surge, like the one expected following neuronal activation, and slowly return to their original size afterward. When two stimuli are presented close together, the vessels' diameter is still dilated close to it maximum capacity by the time the second stimulus is presented, and thus the response to the second stimulus is smaller and has a slightly different shape. This effect was included in the estimation of the balloon model parameters where it is directly related to the poststimulus undershoot. However, the estimation routine did not predict a strong poststimulus undershoot (Fig. 5). While the balloon model explains some of the nonlinearity in the data (as shown in Fig. 5), it is also evident that there remains residual nonlinearities not explained by this venous volume effect and likely to represent nonlinearities at the metabolic and/or neuronal level.

A simple model of canonical nonlinearity

Nonlinearity in BOLD responses can come from a number of sources: neural, vascular, psychophysical, and psychological (e.g., Kileny et al., 1980; Logothetis, 2002, 2003; Raichle et al., 1994; Wilson et al., 1984). Whatever the source of nonlinearities, however, if the goal is accurate prediction of the BOLD response, it is only necessary to measure the end product of nonlinear physiological effects on the BOLD response itself. This consideration has motivated the Volterra series formulation of Friston et al. (1998, 2000), which 'linearizes' sequence effects into a number of linear predictors, and produces very accurate model fits to data, at the cost of statistical power of the overall model, and in particular, the psychological parameters of interest. Calculating nonlinear effects using our model is computationally efficient, and they can be easily incorporated into the linear modeling framework without using up additional degrees of freedom in the model.

Limitations of the current study

Several studies have pointed out that nonlinear effects may differ among brain regions (Birn et al., 2001; Huettel and McCarthy, 2001). We also found some such effects, with small but consistent differences in nonlinear saturation between visual and motor regions. Using an overall average estimate of nonlinear effects prospectively, as we suggest here, is most meaningful if those nonlinearities do not vary with brain region. We find that the overall saturation effects occur in approximately the same form, and these overall effects are several times larger than the saturation × region interactions; thus, we suggest that using the canonical estimates for nonlinear responses we propose may provide a reasonable first-order approximation to estimating nonlinearities. However, the model will provide a poorer fit to brain regions that exhibit noncanonical saturation effects.

The situation is analogous to the difficulties posed by using a canonical estimate of the HRF at all (e.g., Friston et al., 1995a), although this has become common practice in many laboratories. The shape of the hemodynamic response itself is not consistent throughout the brain (Marrelec et al., 2003; Rajapakse et al., 1998), but the canonical form provides a first-order approximation. We provide a "canonical" first-order estimate for nonlinear effects. While nonlinearities surely differ to some degree across brain regions, we hope to provide an average starting point that will reasonably approximate nonlinear effects.

An alternative, or complementary, approach might be to add predictors that represent stimulation history to the design matrix and thus fit a parameter for magnitude × history effects in each brain voxel (this is a simplification of the full Volterra approach). The current estimates could complement this approach if they are used as priors in a Baysian model estimation framework (e.g.,

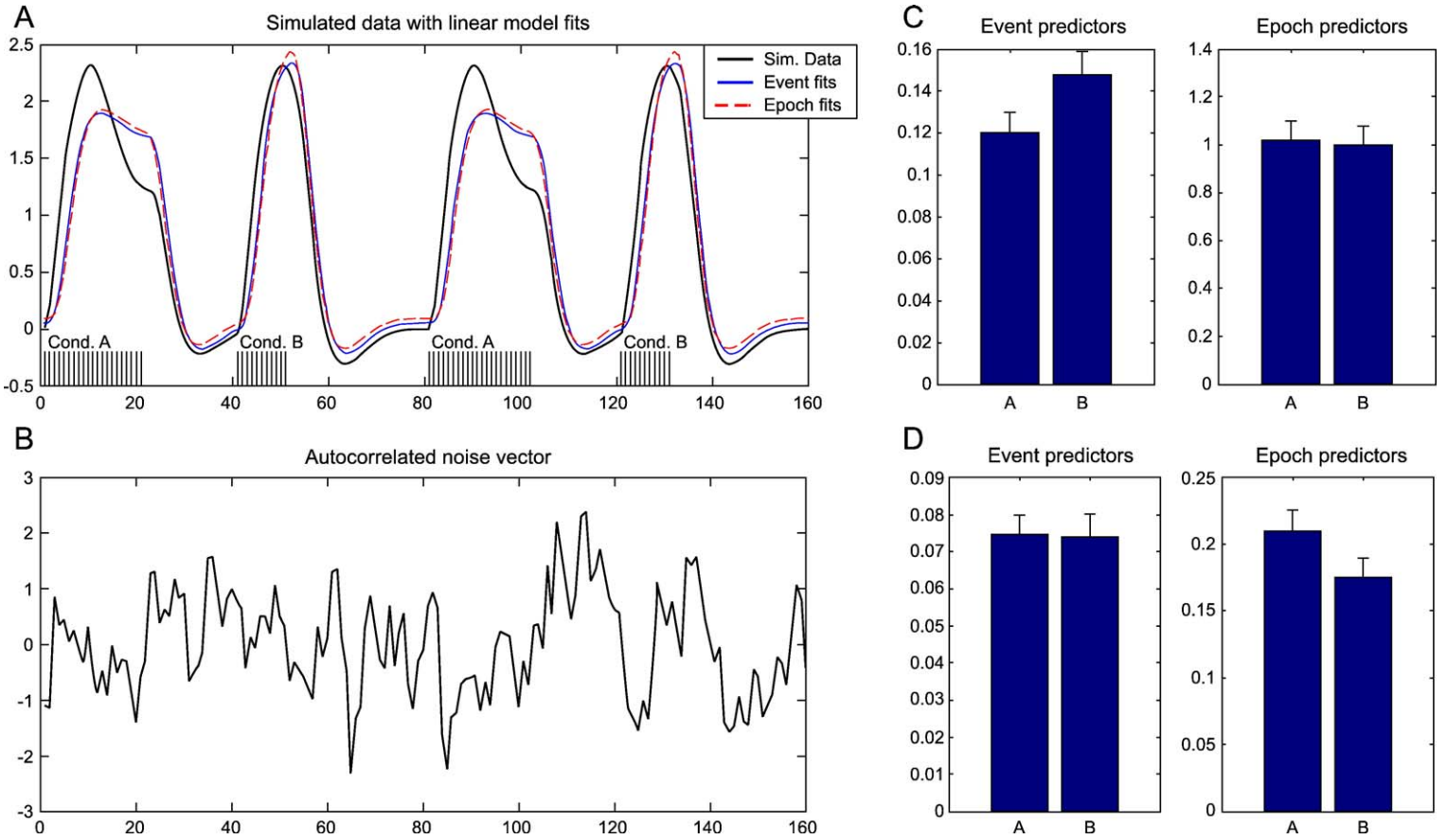

Fig. 7. Simulation showing that artifactual differences between task conditions due to nonlinearities in the BOLD response may occur when comparing blocks of unequal lengths. This is true even when neural activity is identical across conditions and when comparing across participants in a random effects analysis. (A) Simulated data (heavy black line) were created using nonlinear parameter estimates derived from the experiment. Thus, the 'true' response has nonlinearities of the form we report here. 'Neural' events, shown by vertical black lines at the bottom of the figure, occurred every 1 s for both conditions A and B. The assumed hemodynamic response (HRF) to each event was the same for both conditions. The only difference was that condition A consisted of longer blocks (20 s) than condition B (10 s). Models with two regressors (A and B) plus intercept were fit to the data. The "event" model consisted of events (vertical black lines) convolved with the canonical SPM99 HRF for each condition. The "epoch" model consisted of 20 s (condition A) or 10 s (condition B) epochs convolved with the HRF in SPM99. Blue and red lines show overall model fits for both models. (B) Example noise vector. An autocorrelated noise time series with the same variance as the signal (Cohen's $d = 1$), comparable to signal–noise ratios from real experiments, was added to the simulated data. Beta weights were obtained for each condition and the process was repeated for 1000 noise realizations. (C) Beta weights for conditions A and B for the event (left panel) and epoch (right panel) models. As the response to each event was the same for both conditions, beta weights are expected to be the same as well. Estimates differ for the event model, but not the epoch model, indicating an artifactual result for the event model. Estimates are based on 1000 realizations, but error bars are standard errors of the mean based on a sample of 10 participants, comparable to a typical experiment. Nonlinearities in the response caused a systematically smaller response for the 20-s block (condition A), resulting in lower beta weights. (D) Repetition of the simulation with a true response (simulated data) consisting of a linear convolution of events spaced every 3 s, with 20 and 10 s blocks for conditions A and B, respectively. Three seconds was chosen because little nonlinearity is expected to occur at this interval. If the true response is linear, the event model fits accurately, but the epoch model shows an artifactual difference between conditions. Simulations with linear simulated data at 1 s, as in A, showed an even more pronounced effect.

Friston and Penny, 2003; Penny et al., 2003; Smith et al., 2003; Woolrich et al., 2004).

Another limitation of the study is that nonlinear effects were estimated using an ISI of 1 s throughout the experiment, which is suitable for fast ER designs with interstimulus intervals around this length. For example, average response times are near 1 s for many cognitive tasks. This poses a serious limitation, however, as we cannot provide quantitative estimates of nonlinearity at other delay times (e.g., 3–4 s typical of many event-related paradigms). The problem can be approximately solved by assuming a linear or exponential decrease in nonlinear saturation with increasing ISI, as the response is known to be very near linear at ISIs of greater than 5 s (Miezin et al., 2000).

Acknowledgments

We would like to thank John Jonides and Tom Nichols for helpful discussions and comments on the experiment. This research was supported by grant MH60655 to the University of Michigan (John Jonides, P.I.). Software implementing the modified convolution and nonlinearity equations is available from http://www.columbia.edu/cu/psychology/tor/ or by e-mailing tor@psych.columbia.edu.

References

Birn, R.M., Saad, Z.S., Bandettini, P.A., 2001. Spatial heterogeneity of the nonlinear dynamics in the FMRI BOLD response. NeuroImage 14 (4), 817–826.

Birn, R.M., Cox, R.W., Bandettini, P.A., 2002. Detection versus estimation in event-related fMRI: choosing the optimal stimulus timing. NeuroImage 15 (1), 252–264.

Boynton, G.M., Engel, S.A., Glover, G.H., Heeger, D.J., 1996. Linear systems analysis of functional magnetic resonance imaging in human V1. J. Neurosci. 16 (13), 4207–4221.

Buckner, R.L., 1998. Event-related fMRI and the hemodynamic response. Hum. Brain Mapp. 6 (5–6), 373–377.

Burock, M.A., Buckner, R.L., Woldorff, M.G., Rosen, B.R., Dale, A.M., 1998. Randomized event-related experimental designs allow for extremely rapid presentation rates using functional MRI. NeuroReport 9 (16), 3735–3739.

Buxton, R.B., Frank, L.R., 1997. A model for the coupling between cerebral blood flow and oxygen metabolism during neural stimulation. J. Cereb. Blood Flow Metab. 17 (1), 64–72.

Buxton, R.B., Wong, E.C., Frank, L.R., 1998. Dynamics of blood flow and oxygenation changes during brain activation: the balloon model. Magn. Reson. Med. 39 (6), 855–864.

Cohen, M.S., 1997. Parametric analysis of fMRI data using linear systems methods. NeuroImage 6 (2), 93–103.

D'Esposito, M., Postle, B.R., Jonides, J., Smith, E.E., 1999. The neural substrate and temporal dynamics of interference effects in working memory as revealed by event-related functional MRI. Proc. Natl. Acad. Sci. U. S. A. 96 (13), 7514–7519.

Dale, A.M., Buckner, R.L., 1997. Selective averaging of rapidly presented individual trials using fMRI. Hum. Brain Mapp. 5, 329–340.

Davachi, L., Wagner, A.D., 2002. Hippocampal contributions to episodic encoding: insights from relational and item-based learning. J. Neurophysiol. 88 (2), 982–990.

Friston, K.J., Penny, W., 2003. Posterior probability maps and SPMs. NeuroImage 19 (3), 1240–1249.

Friston, K.J., Frith, C.D., Turner, R., Frackowiak, R.S., 1995. Characterizing evoked hemodynamics with fMRI. NeuroImage 2 (2), 157–165.

Friston, K.J., Holmes, A.P., Poline, J.B., Grasby, P.J., Williams, S.C., Frackowiak, R.S., et al., 1995. Analysis of fMRI time-series revisited. NeuroImage 2 (1), 45–53.

Friston, K.J., Josephs, O., Rees, G., Turner, R., 1998. Nonlinear event-related responses in fMRI. Magn. Reson. Med. 39 (1), 41–52.

Friston, K.J., Mechelli, A., Turner, R., Price, C.J., 2000. Nonlinear responses in fMRI: the balloon model, Volterra kernels, and other hemodynamics. NeuroImage 12 (4), 466–477.

Haxby, J.V., Petit, L., Ungerleider, L.G., Courtney, S.M., 2000. Distinguishing the functional roles of multiple regions in distributed neural systems for visual working memory. NeuroImage 11 (2), 145–156.

Henson, R.N., Price, C.J., Rugg, M.D., Turner, R., Friston, K.J., 2002. Detecting latency differences in event-related BOLD responses: application to words versus nonwords and initial versus repeated face presentations. NeuroImage 15 (1), 83–97.

Hernandez, L., Wager, T.D., Jonides, J., 2002. Introduction to functional brain imaging. In: Wixted, J., Pashler, H. (Eds.), Stevens Handbook of Experimental Psychology, vol. 4. John Wiley and Sons, Inc., New York, pp. 175–221.

Huettel, S.A., McCarthy, G., 2001. Regional differences in the refractory period of the hemodynamic response: an event-related fMRI study. NeuroImage 14 (5), 967–976.

Josephs, O., Henson, R.N., 1999. Event-related functional magnetic resonance imaging: modelling, inference and optimization. Philos. Trans. R. Soc. London, B Biol. Sci. 354 (1387), 1215–1228.

Kerns, J.G., Cohen, J.D., MacDonald III, A.W., Cho, R.Y., Stenger, V.A., Carter, C.S., 2004. Anterior cingulate conflict monitoring and adjustments in control. Science 303, 1023–1027.

Kileny, P., Ryu, J.H., McCabe, B.F., Abbas, P.J., 1980. Neuronal habituation in the vestibular nuclei of the cat. Acta Oto-Laryngol. 90 (3–4), 175–183.

Liu, T.T., 2004. Efficiency, power, and entropy in event-related fMRI with multiple trial types. Part II: design of experiments. NeuroImage 21 (1), 401–413.

Liu, T.T., Frank, L.R., 2004. Efficiency, power, and entropy in event-related FMRI with multiple trial types. Part I: theory. NeuroImage 21 (1), 387–400.

Liu, T.T., Frank, L.R., Wong, E.C., Buxton, R.B., 2001. Detection power, estimation efficiency, and predictability in event-related fMRI. NeuroImage 13 (4), 759–773.

Logothetis, N.K., 2002. The neural basis of the blood–oxygen-level-dependent functional magnetic resonance imaging signal. Philos. Trans. R. Soc. London, B Biol. Sci. 357 (1424), 1003–1037.

Logothetis, N.K., 2003. The underpinnings of the BOLD functional magnetic resonance imaging signal. J. Neurosci. 23 (10), 3963–3971.

Logothetis, N.K., Pauls, J., Augath, M., Trinath, T., Oeltermann, A., 2001. Neurophysiological investigation of the basis of the fMRI signal. Nature 412 (6843), 150–157.

MacDonald III, A.W., Cohen, J.D., Stenger, V.A., Carter, C.S., 2000. Dissociating the role of the dorsolateral prefrontal and anterior cingulate cortex in cognitive control. Science 288 (5472), 1835–1838.

Mandeville, J.B., Marota, J.J., Ayata, C., Zaharchuk, G., Moskowitz, M.A., Rosen, B.R., et al., 1999. Evidence of a cerebrovascular postarteriole windkessel with delayed compliance. J. Cereb. Blood Flow Metab. 19 (6), 679–689.

Marrelec, G., Benali, H., Ciuciu, P., Pelegrini-Issac, M., Poline, J.B., 2003. Robust Bayesian estimation of the hemodynamic response function in event-related BOLD fMRI using basic physiological information. Hum. Brain Mapp. 19 (1), 1–17.

Mechelli, A., Price, C.J., Henson, R.N., Friston, K.J., 2003. Estimating efficiency a priori: a comparison of blocked and randomized designs. NeuroImage 18 (3), 798–805.

Miezin, F.M., Maccotta, L., Ollinger, J.M., Petersen, S.E., Buckner, R.L., 2000. Characterizing the hemodynamic response: effects of presentation rate, sampling procedure, and the possibility of ordering brain activity based on relative timing. NeuroImage 11 (6 Pt. 1), 735–759.

Noll, D.C., Cohen, J.D., Meyer, C.H., Schneider, W., 1995. Spiral K-space MR imaging of cortical activation. J. Magn. Reson. Imaging 5 (1), 49–56.

Oppenheim, A.V., Schafer, R.W., Buck, J.R., 1999. Discrete-Time Signal Processing, 2nd ed. Prentice Hall, Upper Saddle River, NJ.

Penny, W., Kiebel, S., Friston, K., 2003. Variational Bayesian inference for fMRI time series. NeuroImage 19 (3), 727–741.

Press, W.H., Teukolski, S.A., Vetterling, W.T., Flannery, B.P., 1992. Numerical Recipes in C: The Art of Scientific Computing. Cambridge University Press, New York.

Raichle, M.E., Fiez, J.A., Videen, T.O., MacLeod, A.M., Pardo, J.V., Fox, P.T., et al., 1994. Practice-related changes in human brain functional anatomy during nonmotor learning. Cereb. Cortex 4 (1), 8–26.

Rajapakse, J.C., Kruggel, F., Maisog, J.M., von Cramon, D.Y., 1998. Modeling hemodynamic response for analysis of functional MRI time-series. Hum. Brain Mapp. 6 (4), 283–300.

Smith, M., Putz, B., Auer, D., Fahrmeir, L., 2003. Assessing brain activity through spatial Bayesian variable selection. NeuroImage 20 (2), 802–815.

Vazquez, A.L., Noll, D.C., 1998. Nonlinear aspects of the BOLD response in functional MRI. NeuroImage 7 (2), 108–118.

Vazquez, A., Noll, D., 2002. A fluid mechanical approach to modeling hemodynamics in fMRI. Paper presented at the 10th Annual Mtg. of the Int. Soc. of Magn. Reson. in Med., Honolulu, HI.

Wager, T.D., Nichols, T.E., 2003. Optimization of experimental design in fMRI: a general framework using a genetic algorithm. NeuroImage 18 (2), 293–309.

Wagner, A.D., Schacter, D.L., Rotte, M., Koutstaal, W., Maril, A., Dale, A.M., et al., 1998. Building memories: remembering and forgetting of verbal experiences as predicted by brain activity. Science 281 (5380), 1188–1191.

Wilson, C.L., Babb, T.L., Halgren, E., Wang, M.L., Crandall, P.H., 1984. Habituation of human limbic neuronal response to sensory stimulation. Exp. Neurol. 84 (1), 74–97.

Woods, R.P., Grafton, S.T., Holmes, C.J., Cherry, S.R., Mazziotta, J.C., 1998. Automated image registration: I. General methods and intra-subject, intramodality validation. J. Comput. Assist. Tomogr. 22, 141–154.

Woolrich, M.W., Jenkinson, M., Brady, J.M., Smith, S.M., 2004. Fully Bayesian spatio-temporal modeling of FMRI data. IEEE Trans. Med. Imag. 23 (2), 213–231.